J of Nuclear Medicine Technology, first published online July 30, 2021 as doi:10.2967/jnmt.121.262415

Renal Cortical Scarring: ^{68}Ga-PSMA-11 PET versus ^{99m}Tc-DMSA Scan in a Case with Pyelonephritis

Ismet Sarikaya[1], Ahmed Alqallaf[2], Ali Sarikaya[3] Ali Baqer[4], Nafisa Kazem[5]

[1]Department of Nuclear Medicine, Kuwait University Faculty of Medicine, Mubarak Al-Kabeer Hospital, Kuwait City, Kuwait

[2]Department of Nephrology, Mubarak Al-Kabeer Hospital, Kuwait City, Kuwait

[3]Department of Nuclear Medicine, Trakya University Faculty of Medicine, Edirne, Turkey

[4]Department of Nuclear Medicine, Mubarak Al-Kabeer Hospital, Kuwait City, Kuwait

[5]Department of Nuclear Medicine, Mubarak Al-Kabeer Hospital, Kuwait City, Kuwait

Correspondence Address:
Ismet Sarikaya, MD ABNM, Professor (Turkey)
Associate Professor,
Department of Nuclear Medicine
Faculty of Medicine, Kuwait University
PO Box 24923
Safat, Kuwait 13110
Phone: (965) 25319592 / 6414
Fax: (965) 25338936
Email: isarikaya99@yahoo.com
Running Title: Renal cortical PSMA PET

ABSTRACT

We previously reported ^{68}Ga-prostate‑specific membrane antigen (PSMA)-11 and ^{99m}Tc-dimercaptosuccinic acid (DMSA) images of the 1st case of our prospective research comparing renal PSMA PET to DMSA scan in adult patients with pyelonephritis. Here, we present renal cortical PSMA PET and DMSA images of our 2nd patient with chronic recurring pyelonephritis which demonstrated renal parenchymal defects secondary to scarring in the kidney.

Key Words: DMSA scan, ^{68}Ga-PSMA-11, PET, pyelonephritis, renal scar

INTRODUCTION

Renal cortical imaging with ^{99m}Tc-dimercaptosuccinic acid (DMSA) scan is widely used to detect renal parenchymal changes due to acute pyelonephritis (reduced uptake) and renal sequelae (scars) (absent uptake) 6 mo after acute infection (1). DMSA scan is also used to quantify differential renal function and detect various renal abnormalities and assess functional status of multicystic kidney (1). Depiction of renal scar via DMSA scan is important because scarring is a common cause of hypertension and extensive scarring can lead to progressive renal impairment and end-stage renal disease (2). Presence of scar can lead to change in treatment plan such as starting different antibiotics, corticosteroids, treating bladder and bowel dysfunction or surgical interventions to prevent further scar formation (3). Potential new treatments such as Cyclooxygenase 2 inhibitors, Superoxide dismutases, matrix metalloproteinase-9 inhibitors may also prevent scar formation (3). Non-functioning or poorly functioning kidney due to chronic recurrent pyelonephritis may be surgically removed as it may cause systemic complications such as sepsis, septic shock, and hypertension (2).

^{68}Ga prostate specific membrane antigen (^{68}Ga-PSMA) ligands or inhibitors are currently used for initial staging of high risk prostate cancer and to identify site of recurrence in the setting of biochemical recurrence (4-6). These radiotracers also exhibit high renal cortical physiological uptake. PSMA is a Type II transmembrane protein, also known as glutamate carboxypeptidase II or folate hydrolase, which is mainly found in prostate tissue and is overexpressed in prostate cancer, some extraprostatic normal tissues such as kidneys and salivary glands and also in various other malignancies (7-9). Immunohistochemical analyses demonstrated detectable PSMA levels in the brush borders and apical cytoplasm of a subset of proximal renal tubules (7,10). The reason

for the presence of PSMA in renal proximal tubules is currently undefined, but may be due to folate metabolism, potential reuptake of folate in the kidneys (11).

We previously published PSMA PET renal cortical images of prostate cancer patients with and without cortical defects caused by various sizes of cysts (2,12,13). Given high renal cortical uptake and excellent renal parenchymal distribution of ^{68}Ga-PSMA-11, we started a prospective research comparing renal PSMA PET to DMSA scan in adult patients with pyelonephritis. Our study was interrupted by Covid-19 pandemic but renal PSMA PET and DMSA images of our first case has been published (14). In our first case, neither PSMA PET nor DMSA scan showed cortical defects but PSMA PET demonstrated superior image quality over DMSA scan. In the current report, we present renal PSMA PET and DMSA images of our second patient which demonstrated cortical defects caused by scars.

METHODS

Our prospective study was approved by the Ethical Committee of Health Sciences Center at Kuwait University and Kuwait Ministry of Health. The study was conducted at Mubarak Al-Kabeer Hospital in Kuwait.

The patient provided written informed consent before the study. We obtained PSMA PET/CT and DMSA images from the kidneys.

Radiolabeling of ^{68}Ga-PSMA ligand (PSMA-11) was carried out at another institute (Radiopharmacy Unit at Kuwait Cancer Control Center) using 68Ge/68Ga generator and a manual synthesis module (Isotope Technologies Garching (ITG), Germany).

Renal PSMA PET/CT images were obtained at Philips Time of Flight PET/CT camera (Philips Medical Systems, Best, Netherlands) 60 min following intravenous injection of 48.1 MBq (1.3 mCi) of ^{68}Ga-PSMA ligand. We intentionally used low activity to reduce radiation dose

to patient. A low-dose, unenhanced CT from region of the kidneys was obtained for attenuation correction, anatomic localization and gross anatomical correlation purposes prior to PET acquisition (30 mAs, 120 KV, 0.829 pitch, 0.5 sec rotation time, 64x0.625 collimation value and 5 mm slice thickness). PET acquisition time was 10 min/bed for 2 beds. Due to low dose activity administration image acquisition time was longer than usual. PET images were corrected for attenuation based on CT data, reconstructed using a standard iterative algorithm and reformatted into transaxial, coronal**,** and sagittal slices. Maximum intensity projection (MIP) images were also generated. Because of intense activity in the kidneys, PET images were reviewed in low intensity setting to better assess renal cortical uptake and distribution. Attenuation corrected (AC), uncorrected (non-AC) PET, PET/CT fusion and low-dose CT images were reviewed to assess the anatomical location, size and morphology of the kidneys, uptake and distribution of radiotracer in the renal parenchyma, and to search for the parenchymal defects and other abnormalities. Quantification of renal PSMA uptake was also performed. Due to unexpected high splenic uptake in this case, we could not use automated VOI analysis with the software we had. Manual region of interest around kidneys in multiple transaxial slices were drawn to calculate total activities in each kidney. In addition, we also measured SUV_{max}, SUV_{mean} in both kidneys in normal and areas with parenchymal defect by placing a spherical region of interest over renal cortex without exceeding renal border.

Four days after PET imaging, DMSA images were obtained 3 hours following intravenous injection of 111 MBq (3 mCi) ^{99m}Tc-DMSA using Symbia S SPECT scanner (Siemens Healthineers, Erlangen, Germany) equipped with a high resolution parallel hole collimator. Multiple planar images were obtained in anterior, posterior, right posterior oblique and left posterior oblique projections (10 minute each, 20% window centered at 140 keV, 256 x 256 matrix

and zoom 1.3). Single photon emission computed tomography (SPECT) images of the kidneys were also obtained (20 second acquisition per view, 60 views, 360° rotation, 128x128 matrix, no zoom, 20% window centered at 140 keV). A standard iterative algorithm was used for image reconstructed. Images were reformatted into transaxial, coronal**,** and sagittal views. Quantification of renal uptake for each kidney was performed using anterior and posterior planar images and geometric mean.

RESULTS

The patient was a 49 year-old female with history of recurring pyelonephritis in the last 14 mos. The last episode was a severe emphysematous pyelonephritis which occurred 2 months prior to this study (positive urine culture for Candida Albicans) which was treated with antibiotics for 1 month as an inpatient treatment. Currently the patient does not have any symptoms and urine culture is negative. Renal Ultrasound taken a month prior to this study demonstrated dilated left renal pelvis and calyces with stones, preserved cortical thickness and corticomedullary differentiation.

Planar and SPECT DMSA images demonstrated cortical defects, reduced uptake, and cortical irregularity in the upper and lower poles of the left kidney (Figure 1). In the right kidney, no cortical defects were identified with only slightly reduced uptake in the upper and lower poles which could be a normal finding.

AC PET images had artifact in the upper pole of the right kidney which seemed secondary to some possible unilateral patient motion as patient passed urine during imaging. AC PET also showed reduced uptake and cortical defects in the upper and lower poles of the left kidney (Figure 2). Splenic uptake was higher than usual in this case likely due to ^{68}Ga-colloid formation. In

normal physiological distribution of ^{68}Ga-PSMA-11 splenic uptake is much lower than renal uptake and do not interfere the interpretation of images (Figure 3).

Non-AC PET images demonstrated similar findings to DMSA scan with cortical defects, reduced uptake and irregularity in the upper and lower poles of the left kidney (Figure 1). In upper and lower poles of the right kidney there was mildly reduced uptake similar to DMSA scan. Bowel activity in the left upper quadrant did not affect the assessment of left kidney, but caused some overlap on left kidney on MIP images. Low dose CT demonstrated small calculi in the lower pole of the left kidney. There were no cysts in the kidneys on low-dose CT.

Renal uptake was 35.5% on the left and 64.5% on the right with DMSA, and 34.5% on the left and 65.5% on the right with PSMA.

SUV_{max} and SUV_{mean} of normal right kidney parenchyma were 53 and 43, respectively. In the left kidney, SUV_{max} and SUV_{mean} in the upper pole were 6.4 and 4, respectively, in the lower pole were 21.6 and 17.6 in and in the mid cortical region were 52 and 41, respectively.

DISCUSSION

DMSA scan is the current gold standard to assess renal parenchyma and detect renal scarring which have been described in detail in our recently published articles (2, 12-14). Identification of renal scar in patents with pyelonephritis is important because scarring is a common cause of hypertension and extensive scarring can cause progressive loss of renal function (2). In the management of patients with scarring due to pyelonephritis, a change in treatment plan such as starting different antibiotics and supporting with other medications, treating bladder and bowel dysfunction or surgical intervention (correcting vesicoureteral reflux) may help preventing further scarring (3). Potential new treatments may also prevent further scar development (3).

There is a shortage of DMSA cold kit in various countries including US and therefore DMSA has been added to the Drug Shortages List of the US FDA in 2014 and is commercially unavailable thereafter (15). Currently, there isn't a good alternative to DMSA scan. ^{99m}Tc-glucoheptonate is only partially concentrated in the kidneys and then excreted in the urine (1). ^{68}Ga-Alizarin Red S was studied in animals and humans as a renal cortical PET radiotracer in 1980s but not used thereafter (16). In a recent meta-analysis study, we compared DMSA scan to magnetic resonance imaging (MRI) and found overall equivalent sensitivity of MRI and DMSA scan in detecting parenchymal changes in pyelonephritis, particularly in scar detection (17). MRI has also certain limitations and is not commonly used in routine to assess cases with pyelonephritis (18). New radiotracers, particularly PET tracers, are needed which can selectively accumulate in renal parenchyma, provide higher resolution images of the kidneys, detect smaller cortical defects and allow better quantification of split renal function as compared to DMSA scan.

In our current case, both PSMA PET (AC and non-AC) and DMSA scan demonstrated cortical defects/scars in the left kidney with a comparable image quality. Due to high splenic uptake from ^{68}Ga-colloid formation and some motion related artifacts in the right kidney, image quality in our current case was lower as compared to PSMA PET images of our previously reported case (14) (Figure 3). During the labeling procedure, formation of ^{68}Ga-colloid may occur and ^{68}Ga-colloid will accumulate in the spleen, liver and bone marrow (19). Thin layer chromatography (TLC) method is used to measure colloid content. We did not repeat the PSMA PET study in this case because we did not want our patient to receive additional radiation exposure. Although splenic uptake and some motion on the right side, AC and non-AC images successfully demonstrated scars in the left kidney.

Studies have demonstrated a good correlation between renal DMSA uptake and renal function tests, such as effective renal plasma flow (ERPF), glomerular filtration rate (GFR) and creatinine clearance (20-24). In our recently submitted retrospective study in 25 prostate cancer patients, renal ^{68}Ga-PSMA-11 uptake appears to be correlating well with the renal function tests (creatinine and GFR).

There are certain advantages of PSMA PET over DMSA scan such as shorter waiting time after injection (1 hr versus 3 hr), shorter half-life (68 min vs 6 h) and superior image quality, particularly with AC PET. Image acquisition time in our current case was 20 min with PSMA PET because we used low-dose activity to reduce radiation dose to patient (2 bed, 10 min/bed, 48.1 MBq (1.3 mCi)). Image acquisition time with DMSA scan was 45 minutes (20 min planar, 25 min SPECT). Longer acquisition time can cause patient discomfort and patient motion resulting with image artifacts, requiring additional images and sedation in pediatric patients. Image acquisition time with PSMA PET can be further reduced to 6-7 min/bed for 74 MBq (2 mCi), 4-5 min/bed for 111 MBq (3 mCi), and 2-3 min/bed with 148 MBq (4 mCi) activities but kidney and effective doses will increase with higher activities. As we reported in our previous articles, absorbed adult kidney doses of ^{68}Ga-PSMA-11 and ^{99m}Tc-DMSA are 0.24 mGy/MBq and 0.18 mGy/MBq, respectively, and effective adult doses of ^{68}Ga-PSMA-11 and ^{99m}Tc-DMSA are 0.022 mSv/MBq and 0.0088 mSv/MBq, respectively (25, 26). In our previously reported case, estimated effective doses of 111 MBq (3 mCi) of ^{99m}Tc-DMSA and 74 MBq (2 mCi) of ^{68}Ga-PSMA-11 were 0.98 mSv and 1.63 mSv, respectively. In our current case , 48.1 MBq (1.3 mCi) ^{68}Ga-PSMA-11 yields an effective dose of 1.05 mSv which is similar to effective dose of DMSA. The additional radiation dose from CT in PET/CT is low because it is a low-dose CT and only covers the region of kidneys. Non-AC PET also provide high quality images of the renal

parenchyma as seen in our current case and in previous reports and therefore low-dose CT can be omitted.

PET/CT cameras provide higher resolution images over standard gamma cameras. Even low-dose non-AC PET provided higher quality or comparable images to DMSA SPECT in our case. SPECT/CT provides higher resolution images than SPECT, but we intentionally did not perform SPECT/CT in our case to reduce radiation dose in this research patient. Overall, PET/CT is known to provide higher resolution images than SPECT/CT. On the other hand, SPECT systems with cadmium zinc telluride (CZT) detectors have better resolution than conventional scanners with sodium iodide detectors (27).

The usage and availability of 68Ga-PSMA ligands for prostate cancer have been increasing. Recently, ^{68}Ga-PSMA-11 has been approved by FDA for prostate cancer imaging. One of the limitations of PSMA PET is its higher cost as compared to DMSA scan. The costs of PSMA PET and DMSA scan are approximately $450 and $300 in our institute.

Quantification of renal uptake for each kidney showed similar results with DMSA scan and PSMA PET. Due to high splenic uptake and limitations in our software we could not perform automated VOI analysis on PSMA images but in our recently submitted study, automated VOI analysis successfully provided total counts, volume, SUVs in each kidney.

In our current case and previous case with chronic pyelonephritis, PSMA PET appears to be a potential alternative to DMSA scan. As discussed in our previous case, its biodistribution and radiation dose in pediatric population is not known and further work is required to understand its mechanism of uptake, to determine optimal injected activity, and dosimetry, before its use as renal cortical tracer can be supported.

CONCLUSION

^{68}Ga-PSMA-11 PET well demonstrated the renal cortical scars caused by pyelonephritis.

DISCLOSURE

^{68}Ga-PSMA ligands are investigational PET radiotracers and as of now they have not been approved by the US Food and Drug Administration and European Medicines Agency. This is off-label use of ^{68}Ga-PSMA ligands for renal imaging.

No potential conflict of interest relevant to this article was reported.

REFERENCES

1. Mandell GA, Eggli DF, Gilday DL, et al. Procedure guideline for renal cortical scintigraphy in children. Society of Nuclear Medicine. *J Nucl Med.* 1997;38:1644-6.
2. Sarikaya I, Sarikaya A. Current status of radionuclide renal cortical imaging in pyelonephritis. *J Nucl Med Technol.* 2019;47:309-312.
3. Murugapoopathy V, McCusker C, Gupta IR. The pathogenesis and management of renal scarring in children with vesicoureteric reflux and pyelonephritis. *Pediatr Nephrol.* 2020;35:349-357.
4. Afshar‐Oromieh A, Avtzi E, Giesel FL, et al. The diagnostic value of PET/CT imaging with the (68)Ga‐labelled PSMA ligand HBED‐CC in the diagnosis of recurrent prostate cancer. *Eur J Nucl Med Mol Imaging.* 2015;42:197‐209.
5. Sonni I, Eiber M, Fendler WP, et al. Impact of (68)Ga-PSMA-11 PET/CT on staging and sanagement of prostate cancer patients in various clinical settings: A Prospective single center study. *J Nucl Med.* 2020 Jan 10. pii: jnumed.119.237602. doi:2967/jnumed.119.237602.
6. Fendler WP, Eiber M, Beheshti M, et al. (68)Ga-PSMA PET/CT: Joint EANM and SNMMI procedure guideline for prostate cancer imaging: version 1.0. *Eur J Nucl Med Mol Imaging.* 2017 ;44:1014-1024.
7. Silver DA, Pellicer I, Fair WR, Heston WD, Cordon-Cardo C. Prostate-specific membrane antigen expression in normal and malignant human tissues. *Clin Cancer Res.* 1997;3:81-5.
8. Mhawech-Fauceglia P, Zhang S, Terracciano L, et al. Prostate-specific membrane antigen (PSMA) protein expression in normal and neoplastic tissues and its sensitivity

and specificity in prostate adenocarcinoma: an immunohistochemical study using mutiple tumour tissue microarray technique. *Histopathology*. 2007;50:472-83.

9. Cunha AC, Weigle B, Kiessling A, Bachmann M, Rieber EP. Tissue-specificity of prostate specific antigens: comparative analysis of transcript levels in prostate and non-prostatic tissues. *Cancer Lett.* 2006;236:229-38.

10. Baccala A, Sercia L, Li J, Heston W, Zhou M. Expression of prostate-specific membrane antigen in tumor-associated neovasculature of renal neoplasms. *Urology*. 2007;70:385-90.

11. Ristau BT, O'Keefe DS, Bacich DJ. The prostate-specific membrane antigen: lessons and current clinical implications from 20 years of research. *Urol Oncol.* 2014;32:272-9.

12. Sarikaya I, Elgazzar AH, Alfeeli MA, Sarikaya A. Can gallium-68 prostate-specific membrane antigen ligand be a potential radiotracer for renal cortical positron emission tomography imaging? *World J Nucl Med.* 2018;17:126-129.

13. Sarikaya I. (68)Ga-PSMA Ligand as Potential (99m)Tc-DMSA Alternative. *J Nucl Med.* 2019;60:12N.

14. Sarikaya I, Alqallaf A, Sarikaya A. Renal cortical 68Ga-PSMA-11 PET and 99mTc-DMSA images. *J Nucl Med Technol.* 2021;49:30-33.

15. Lim R, Bar-Sever Z, Treves ST. Is availability of 99mTc-DMSA insufficient to meet clinical needs in the United States? A survey. *J Nucl Med.* 2019;60:14N–16N.

16. Schuhmacher J, Maier-Borst W, Wellman HN. Liver and kidney imaging with Ga-68 labeled dihydroxyanthraquinones. *J Nucl Med*. 1980;21:983-987.

17. Sarikaya I, Albatineh AN, Sarikaya A. 99mTc-dimercaptosuccinic acid scan versus MRI in pyelonephritis: a meta-analysis. *Nucl Med Commun.* 2020;41:1143-1152.

18. Mervak BM, Altun E, McGinty KA, et al. MRI in pregnancy: Indications and practical considerations. *J Magn Reson Imaging.* 2019;49:621-631.

19. Brom M, Franssen GM, Joosten L, Gotthardt M, Boerman OC. The effect of purification of Ga-68-labeled exendin on in vivo distribution. *EJNMMI Res.* 2016;6:65.

20. Taylor A Jr, Kipper M, Witztum K. Calculation of relative glomerular filtration rate and correlation with delayed technetium-99m DMSA imaging. *Clin Nucl Med.* 1986;11:28-31.

21. Taylor A: Quantitation of renal function with static imaging agents. *Semin Nuci Med* 1982;12:330-344

22. Kawamura J, Hosokawa S, Yoshida O, et al. Validity of 99mTc dimercaptosuccinic acid renal uptake for an assessment for individual kidney function. *J Urol.* 1978;119:305-9.

23. Daly MJ, Jones W, Rudd TG, Tremann J. Differential renal function using technetium-99m dimercaptosuccinic acid (DMSA): in vitro correlation. *J Nucl Med.* 1979;20:63-6

24. Groshar D, Embon OM, Frenkel A, Front D. Renal function and technetium-99m-dimercaptosuccinic acid uptake in single kidneys: the value of in vivo SPECT quantitation. *J Nucl Med.* 1991;32:766-8.

25. Mattsson S, Johansson L, Leide Svegborn S, et al. Radiation dose to patients from radiopharmaceuticals: a Compendium of current information related to frequently used substances [published correction appears in *Ann ICRP*. 2019;48:96] [published correction appears in *Ann ICRP*. 2019;48:97]. *Ann ICRP*. 2015;44:7-321.

26. Sandgren K, Johansson L, Axelsson J, et al. Radiation dosimetry of [^{68}Ga]PSMA-11 in low-risk prostate cancer patients. *EJNMMI Phys*. 2019;6:2.

27. Daghighian F, Sumida R, Phelps ME. PET imaging: An overview and instrumentation. *J Nucl Med Technol.* 1990;18:5-13

Figure 1: ^{99m}Tc-DMSA planar (posterior, and left posterior oblique), and SPECT (MIP in posterior view and selected coronal slice), and ^{68}Ga-PSMA-11 (non-AC MIP in posterior view and non-AC selected coronal slice) demonstrating cortical defects/scars and reduced uptake in upper and lower poles of the left kidney. Note higher image resolution of non-AC PET over non-AC SPECT.

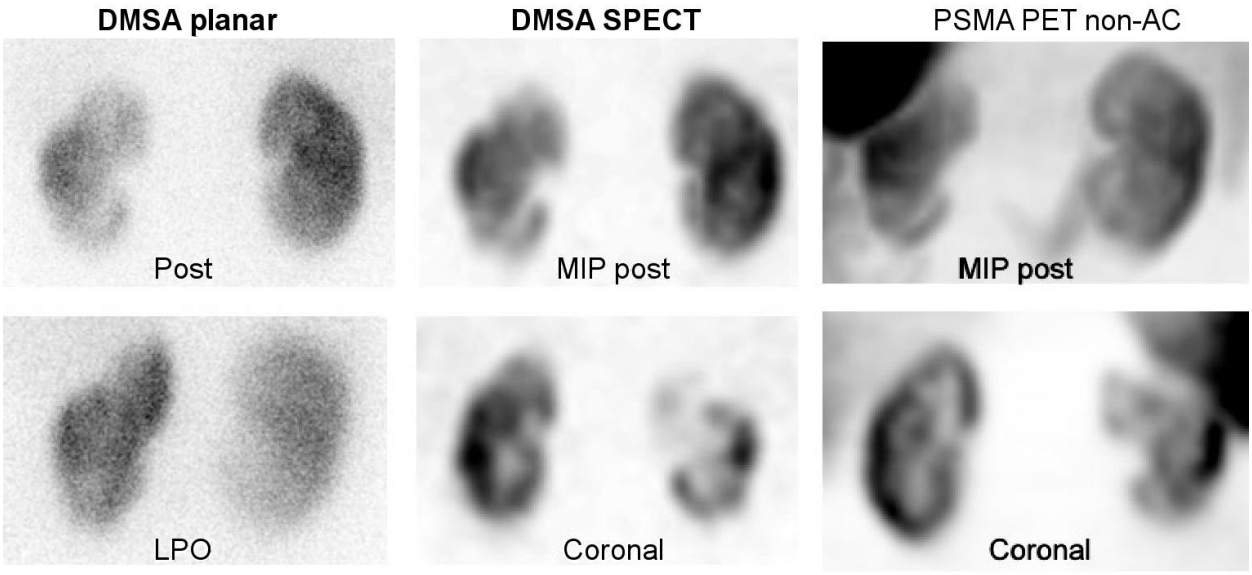

Figure 2: ^{68}Ga-PSMA-11 PET/CT (selected transaxial CT, PET and AC PET/CT fusion) images at lower renal pole level demonstrating reduced uptake in the lower pole of the left kidney and a small cortical defect.

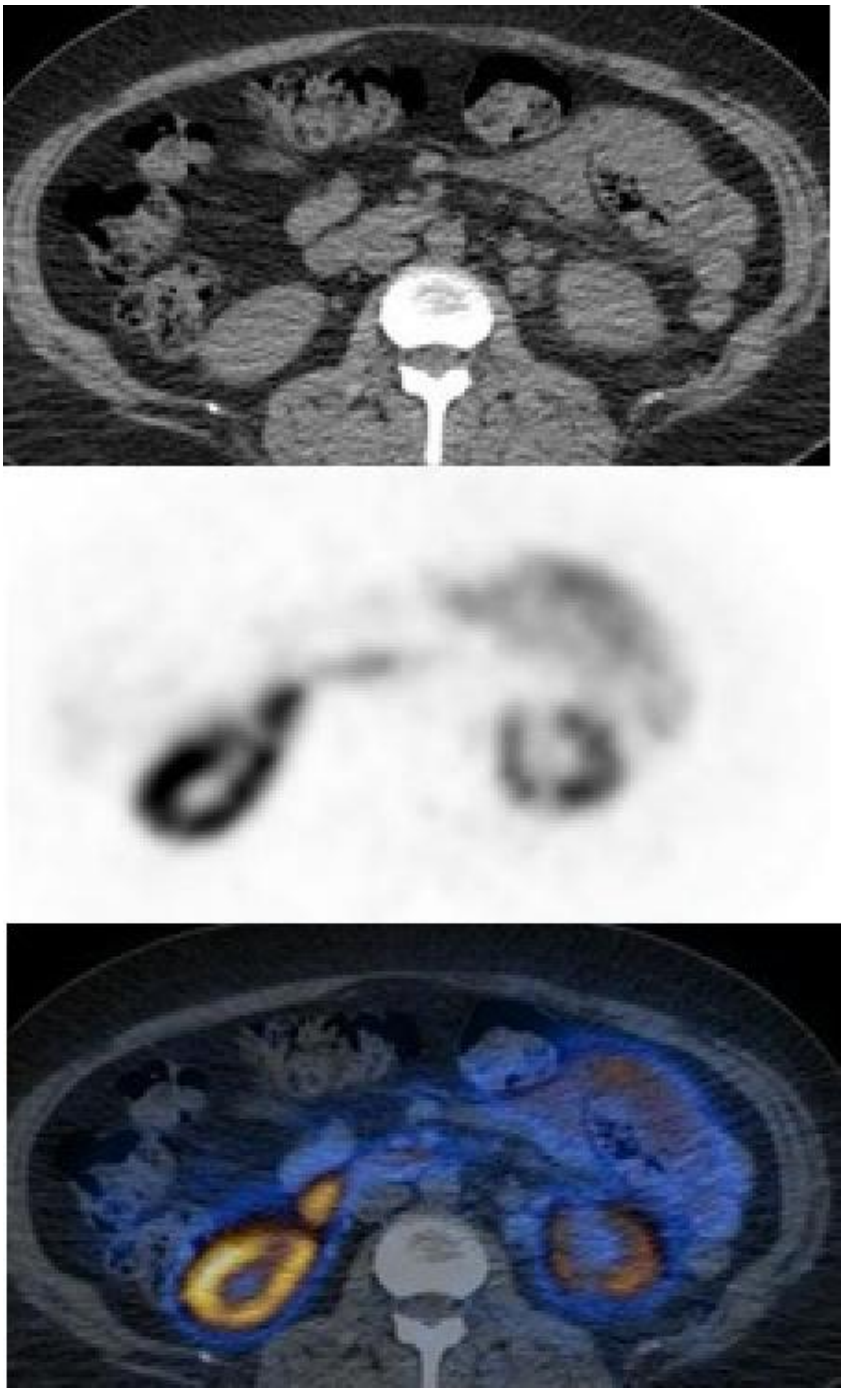

Figure 3: ^{99m}Tc-DMSA SPECT (selected coronal slice), and ^{68}Ga-PSMA-11 PET (AC and non-AC selected coronal slices) images of another case with history of chronic recurrent pyelonephritis demonstrating mildly reduced uptake and cortical thinning in the upper pole of the right kidney with no parenchymal defects. Note the normal distribution of ^{68}Ga-PSMA-11 with only mild activity in the liver and spleen.